ChemComm

Heterostructures of $Cu_{2-x}S/Cu_{2-x}Te$ plasmonic semiconductors: Disappearing and reappearing LSPR with anion exchange

Journal:	*ChemComm*
Manuscript ID	CC-COM-03-2022-001859.R2
Article Type:	Communication

COMMUNICATION

Heterostructures of $Cu_{2-x}S/Cu_{2-x}Te$ plasmonic semiconductors: Disappearing and reappearing LSPR with anion exchange

Received 00th January 20xx,
Accepted 00th January 20xx

DOI: 10.1039/x0xx00000x

Alba Roselia Espinosa,[a] Marc Novak,[a] Qi Luo,[a] Brandon Hole,[a] Clarisse Doligon,[a] Kenya Prenza Sosa,[a] Jennifer L. Gray,[b] Daniel P. Rossi,[c] and Katherine E. Plass [*a]

Localized surface plasmon resonance (LSPR) of $Cu_{2-x}S$ nanorods is quenched during the initial $Cu_{2-x}S/Cu_{2-x}Te$ core/shell stage of anion exchange. LSPR returns as $Cu_{2-x}Te$ progresses into the nanorod despite slight changes in composition. Exchange-induced phase change within the core accounts for this behaviour illustrating the complexity emergent from anion exchange.

Plasmonic nanoparticles—particles wherein the resonant oscillation of free carriers enhances the electric field at the particle surface—have transformed numerous fields. Plasmonic nanoparticles improve the efficiency of solar cells[1] and photocatalysis.[2,3] The strong electric fields produced can drive chemical reactions.[4,5] The wavelength of this localized surface plasmon resonance (LSPR) can be altered by changing the size or shape of the plasmonic nanoparticle, as well as the dielectric constant of the surface.[6,7] This leads to a responsivity to environmental factors which can be employed to design sensors,[8] while the enhancement of surface electric fields is the basis of surface-enhanced Raman spectroscopy (SERS).[9]

Copper chalcogenides are a complex class of NIR plasmonic semiconductors, that can simultaneously exhibit plasmonic and excitonic features.[10,11] LSPR in this system is responsive to particle size[12–15] and shape,[14,16,17] aggregation,[16] surface chemistry,[14,18] and solvent environments,[11,19] as well as alteration of free carrier concentration.[10,11,20–22] Resulting NIR LSPR has been utilized in medical applications.[23,24] Non-stoichiometric copper chalcogenides develop large free hole concentrations, often as a result of large Cu^+ vacancy concentrations[20,21] sustained by altering oxidation states.[25,26] Numerous different chemical species alter the position of the LSPR wavelength through oxidation or reduction.[10,17,21,22] Modelling of LSPR reproduced observed spectra for systems with various shapes of copper chalcogenide.[15,17,27–29]

While LSPR of copper chalcogenide nanoparticles with a single plasmonic component is well studied, heterostructures composed of multiple plasmonic components have received less attention despite the potential for new synergistic behaviours.[30] Au/Cu_2S core/shell nanoparticles show broadening of the Au plasmon band attributed to coupling between the Au plasmon and Cu_2S exciton.[31] $Cu_{2-x}S/Cu_{2-x}Se$ heterojunction particles have been reported,[32,33] but the optical absorption has not been addressed systematically. Thus, the detailed study of Cu_2S-based heterostructures may provide insight into a new class of plasmonic nanoparticles with interesting and useful properties. We recently discovered how to create a variety of $Cu_{2-x}S/Cu_{2-x}Te$ heterostructures through anion exchange of nanorods from $Cu_{2-x}S$ to $Cu_{2-x}Te$.[34] This exchange proceeds without significant disruption of the particle size or shape, despite the usual tendency toward void formation or particle deformation that is usually observed with anion exchange. Partial conversion resulted in distinct placements of $Cu_{2-x}S$ and $Cu_{2-x}Te$ (Fig. 1), providing a novel system for exploring the effects of nanoheterostructure formation between two plasmonic semiconducting materials. This system allows us to evaluate the impact of core/shell formation on the optical behaviour as the nanorods change from $Cu_{2-x}S$, to $Cu_{2-x}S$ with a shell of $Cu_{2-x}Te$ (stages 1 & 2). As the exchange progresses, the $Cu_{2-x}S$ core is broken up into irregular domains (stage 3) and then into a double-dot-in-rod structure (stage 4) where the cores get smaller and smaller until they disappear completely (stage 5). This progression enables us to evaluate size effects of $Cu_{2-x}S$ cores on LSPR, as well as possible core-core coupling effects.[35]

Our study began by examining two extremes of anion exchange progression. Aliquots were removed throughout the reaction at 200 °C (Fig. 2a) and 260 °C (Fig. 2b) and the visible/NIR absorption spectra were measured (Experimental details in SI). Previous experiments[34] demonstrated that anion exchange progresses slowly at 200 °C. Anion exchange starts

[a] Department of Chemistry, Franklin & Marshall College, Lancaster, Pennsylvania 17604, United States.
[b] Materials Research Institute, The Pennsylvania State University, University Park, Pennsylvania 16802, United States.
[c] Department of Chemistry, University of Michigan, Ann Arbor, Michigan 48109, United States.

Electronic Supplementary Information (ESI) available: Experimental information, acknowledgements, and additional data. See DOI: 10.1039/x0xx00000x
Electronic Data Repository: osf.io/vxmjk

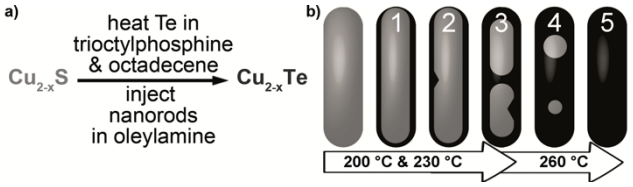

Fig. 1. a) Reaction for conversion of $Cu_{2-x}S$ nanorods to $Cu_{2-x}Te$ nanorods via anion exchange. B) Depiction of the different nanoheterostructures that evolve upon partial anion exchange of $Cu_{2-x}S$ (grey) to $Cu_{2-x}Te$ (black) observed at different temperatures.[34]

with $Cu_{2-x}S/Cu_{2-x}Te$ core/shell nanorods (stage 1) that grow increasingly thick and uneven shells (stage 2) and, after 1 hour, ends with heterostructures in which $Cu_{2-x}Te$ domains extend across the rod (stage 3) (Fig. 1). Visible/NIR spectra monitored from 5 min to 120 min at 200 °C showed four regimes at this low extent of exchange (Fig. 2a). Before anion exchange, $Cu_{2-x}S$ nanorods show band gap absorption around 800 nm (1.4 eV) and a broad plasmon that extended from 900 nm past 2100 nm. To rule out processes such as metal-to-ligand or intervalence charge transfer as the origin of the broad NIR peak, spectra of spheres and rods were compared. The resulting peak shift in response to shape change is indicative of LSPR (Fig. S1). Further confirmation comes from the shift in the peak with increasing hole concentration as a result of oxidation by I_2 (Fig. S2). Immediately upon anion exchange (5 min), plasmon absorption was quenched and a band gap shifted to 1600 nm (0.5 eV). This absorption profile was maintained at 10 min and 20 min and is shows a band gap lower than is typical of stoichiometric Cu_2S (1.1 eV).[36] The 40 min aliquot showed a significant band gap shift to 900 nm (1.2 eV) onset but no plasmon absorbance, which is consistent with stoichiometric Cu_2S. Above 40 min (at 60 min and 120 min), the band gap absorption is unchanged but a plasmon absorbance grows in with a maximum at ~1600 nm. At this point, the absorption behaviour is similar to non-stoichiometric $Cu_{2-x}S$ such as djurleite or roxbyite.[21,36]

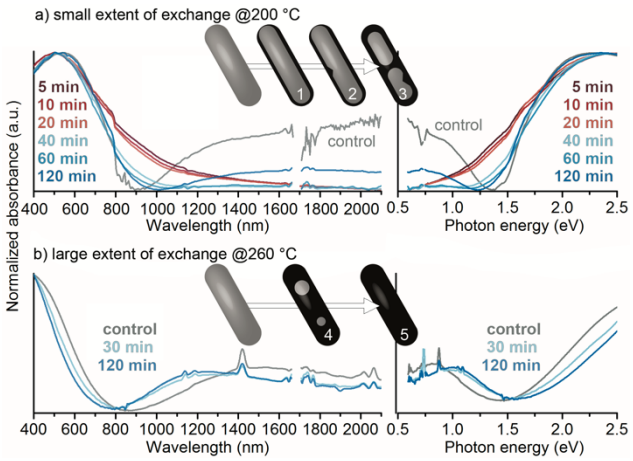

Fig. 2. Visible/NIR absorption spectra of $Cu_{2-x}S$ nanorods that have undergone anion exchange to varying extents through reaction at 200 °C (a) or 260 °C (b) for different times. Overlaid schemes ($Cu_{2-x}S$ grey, $Cu_{2-x}Te$ black) show the expected progression.[34]

Anion exchange proceeds much more rapidly at 260 °C, creating a $Cu_{2-x}S/Cu_{2-x}Te$ double-core structure (stage 4, 20 min-1 hour) that is fully exchanged after 2 hours (stage 5).[34] Surprisingly, visible/NIR spectra of samples at 260 °C showed little alteration despite much greater changes in structure and composition than at 200 °C (Fig. 2b). The band gap onset at 800 nm (1.5 eV) and a plasmon resonance at 1200 nm are similar to the reported spectra of $Cu_{2-x}Te$.[9,17] Initial observations (Fig. 2) raise questions pertinent to understanding the behaviour of multicomponent plasmonic semiconductor systems. Why is the LSPR quenched at early stages of anion exchange (Fig. 2a)? Why doesn't embedding $Cu_{2-x}S$ cores alter the absorption of primarily $Cu_{2-x}Te$ rods, as in Fig. 2b? Several factors must be considered to explain the observed changes in the optical absorption, such as the dielectric constant of the surroundings, the size and shape of the dots within the rods, and the number of free carriers (which can depend on phase in copper chalcogenides).

Throughout the anion exchange process, the overall size of the particles is unchanged (42 nm x 20 nm, Fig. S3) but $Cu_{2-x}S$ domains shrink and change shape.[34] The lattice expansion $Cu_{2-x}Te$ with respect to that of $Cu_{2-x}S$ (by ~6%), is not distinguishable even upon complete exchange. LSPR of the double-core heterostructure (stage 4) might be expected to alter as either the size of the $Cu_{2-x}S$ cores get smaller or as they separate due to decreased coupling.[35] While decreasing $Cu_{2-x}S$ nanoparticle diameters has been reported to shift LSPR wavelength,[12,13] $Cu_{2-x}Te$ is reportedly insensitive to the size of the $Cu_{2-x}Te$ domain.[27] This was attributed to the greater localization of the charge carriers in $Cu_{2-x}Te$ and a weaker plasmonic response.[17] The insensitivity of LSPR to the size of the embedded $Cu_{2-x}S$ cores observed here (Fig. 2b) demonstrates that the holes are quite localized in this system as well.

Later stages of anion exchange were notable for the observed insensitivity of LSPR to the $Cu_{2-x}S/Cu_{2-x}Te$ double core/shell structure (Fig. 2b); the early single $Cu_{2-x}S/Cu_{2-x}Te$ core/shell stage was surprising for the abrupt quenching of LSPR followed by a return of LSPR (Fig. 2a). The rapidity of LSPR quenching on exposure of the $Cu_{2-x}S$ nanorods to the Te/trioctylphosphine reaction solution suggested that surface chemistry may be playing an important role. A control experiment (Fig. S4) showed that the LSPR peak blue shifts when $Cu_{2-x}S$ nanorods are subject to anion exchange conditions in the absence of Te. This confirms that the anion exchange reaction is essential to the observed LSPR quenching and suggests that somehow the initial core/shell formation is responsible for quenching.

Visible/NIR spectroscopic observations coupled with TEM-EDS mapping (Fig. 3) suggests that the disappearance and reappearance of LSPR was tied to a subtle change in the nanoheterostructures. The initial LSPR quenching observed at 200 °C (Fig. 2a) was reproduced more rapidly at 230 °C (Fig. 3). At 5 min, the large LSPR peak at 1600 nm has disappeared and a smaller band gap is observed (Figs. 3a,b). With further anion exchange, the band gap increases (20 min) but the LSPR peak does not return until (35 min and above). TEM-EDS mapping of the 5, 20, 35, and 65 min samples (Figs. 3 f-i) showed subtle differences in the core/shell structure. The amount of Te incorporated steadily increased with time based on the Te/S mole ratio (Fig. 3c) and Cu/Te mole ratios (Fig. 3d). For all samples, most of the $Cu_{2-x}Te$ remains in the shell surrounding the $Cu_{2-x}S$ core; the only difference appears to be the in-roads $Cu_{2-x}Te$ has made perpendicular to the side of the rods. Both samples that do

not exhibit LSPR have more smoothly distributed $Cu_{2-x}Te$ shells (5 min, Figs. 3f and S4 and 20 min, Figs. 3g and S5). The plasmonic $Cu_{2-x}S/Cu_{2-x}Te$ heterostructure at 35 min (Figs. 3h and S6) is similar to the non-plasmonic $Cu_{2-x}S/Cu_{2-x}Te$ heterostructure at 20 min (Figs. 3g and S7) but the shell is less

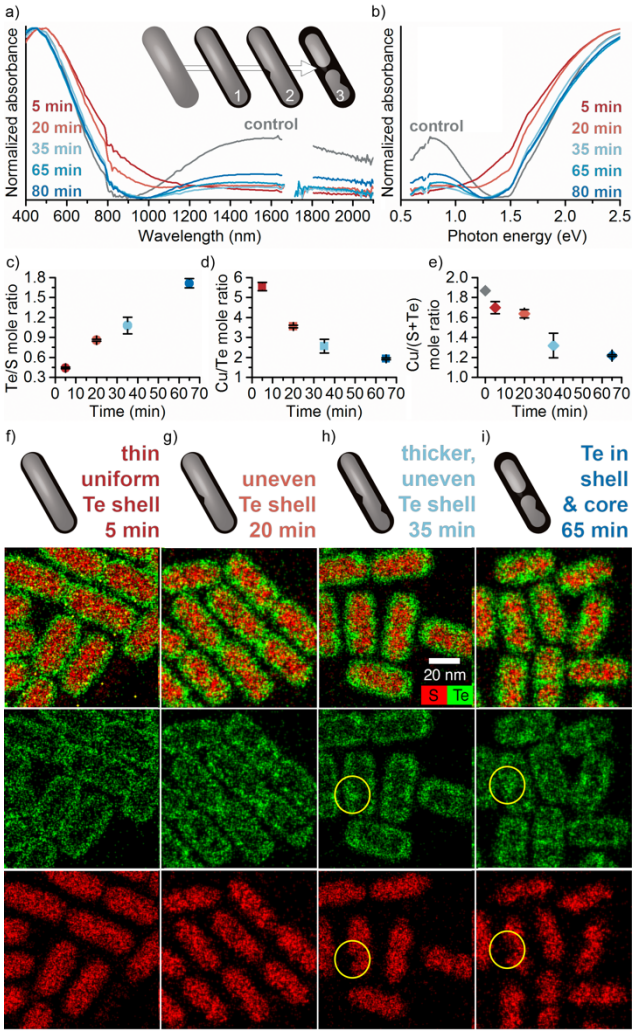

Fig. 3. Characterization of $Cu_{2-x}S$ nanorods that have undergone anion exchange to varying extents through reaction at 230 °C for different times. a,b) Visible/NIR absorption spectra show that the LSPR of the rods before reaction (grey) is quenched at early times (reds) before returning at later times (blues). c,d,e) Mole ratios obtained from TEM-EDS maps show incorporation of Te and replacement of S. f,g,h,i) TEM-EDS maps at various times showing the progression of Te into the core of the rods.

uniform. This is most noticeable in the Te and S maps, where accumulations of Te (yellow circles) occur, accompanied by corresponding lack of S (Figs. 3h and S6). These accumulations increase and start to cross the particles at 65 min (Figs. 3i and S9). The small range in extent over which LSPR quenching occurs and the subtly of the heterostructure alterations rules out a few possible causes of this quenching. Filling of holes in the valence band of $Cu_{2-x}S$ by charge transfer from higher-energy $Cu_{2-x}Te$ valence band should occur regardless of slight alterations in the position of the two materials. Similarly, effects due to differences in the dielectric functions of the two materials should be insensitive to such small changes in geometry.

The increase in copper-deficiency apparent in the EDS data (Figs. 3c-e) appears to rule out the most common cause of LSPR quenching in copper chalcogenides, the formation of stoichiometric phase. Stoichiometric copper chalcogenides are not plasmonic due to a lack of holes—removal of Cu^+ ions to create non-stoichiometric phases results in both creation of free carriers and removal of states at the valence band edge that increase the band gap. If this is causing the observed LSPR quenching, then the composition should show a move towards an integer mole ratio of Cu/(S+Te) stoichiometry. Instead, the mole ratio of Cu to total anion suggests that the particles are becoming more copper-deficient as anion exchange progresses, and all exchanged particles are, on average, more copper-deficient than the initial $Cu_{2-x}S$ starting material (Fig. 3e). The shifted band gap that accompanies LSPR quenching, however, is consistent with the Moss-Burstein effect previously observed for $Cu_{2-x}S$[1] where the band gap decreases as x decreases.

To assess whether LSPR quenching with anion exchange could be caused by formation of a stoichiometric $Cu_{2-x}S$ phase, we coupled observations of visible/NIR spectra (Fig. S10) with PXRD (Fig. 4b). PXRD revealed that despite an overall increase in copper-deficiency as anion exchange progresses (Figs. 3c-e), the diffraction pattern of a non-plasmonic sample matches that of non-stoichiometric α-chalcocite (Fig. 4a). Note the shift of the prominent diffraction peaks in the initial $Cu_{2-x}S$ rods (46.3 and 48.7 °2θ) to lower 2θ (45.8 and 48.4 °2θ) upon exchange (Fig. 4a). This is indicative of an expansion of the d-spacing required to accommodate increasing amounts of Cu^+. This transformation suggests that as Te^{2-} accumulates at the surface and replaces S^{2-}, there is a movement of Cu^+-ions out of the Te-containing layer. These Cu^+ ions leave the particle, leading to an overall decrease in the mole ratio of Cu/(S+Te) (Fig. 3e), but also move into the core where they fill the vacancies leading to the observed phase transformation. Notably, while the Te/S and Cu/Te mole ratios have steady progression with reaction time (Figs. 3c,d), the Cu/(S+Te) mole ratio is unchanged within experimental error for the two non-plasmonic samples (Fig. 3e). This supports the supposition that Cu^+ ions are being retained in a stoichiometric copper sulphide core at early extents of anion exchange, resulting in non-plasmonic particles. As the anion exchange continues, the crystalline phase becomes weissite $Cu_{2-x}Te$ and the total amount of Cu drops to the point where both core and shell are copper-deficient and have sufficient free holes to sustain LSPR (Fig. 4c). Cyclic voltammetry and evaluation of the spectra after oxygen exposure provide further support for the formation of a stoichiometric phase (Figs. S10 and S11) as does LSPR, PXRD, and EDS at lower temperatures (Fig. S12).

Creation of complex nanoheterostructures through processes such as seeded growth and partial cation exchange has revolutionized the nanomaterials field and afforded a large variety of interdependent optical and electronic properties. Here we demonstrate that partial anion exchange between copper chalcogenides is similarly important synthetic tool that induces unexpected optical behaviours worthy of further study and broad application. LSPR of $Cu_{2-x}S/Cu_{2-x}Te$ nanoheterostructures formed during anion exchange from $Cu_{2-x}S$ nanorods to $Cu_{2-x}Te$ nanorods was initially quenched but then reappeared as the extent of anion exchange progressed. Quenching was attributable

to a heterostructure-induced phase-transition to a stoichiometric copper sulphide. This presents a new mechanism for heterostructure-based plasmon switching; previously shell formation has switched off LSPR by state mixing[37] or surface passivation.[38] This behaviour has implications for the use of heterostructured copper chalcogenides for optical, sensing, and thermoelectric applications and it exemplifies the unexpected properties emergent from joining multiple materials within one particle with particular geometries. Specific applications of the $Cu_{2-x}S/Cu_{2-x}Te$ formation technique demonstrated here may include improving the performance of Cu_2S/CdS photovoltaics with stoichiometric phases of Cu_2S[39] or photocatalysis at junctions by Cu^+ trapping.[40] Copper sulphides are common basis for creation of elaborate heterostructures due to cation exchange.[41] Nanostructured $Cu_{2-x}S/Cu_{2-x}Te$ rods can now be used to create yet more complex particles with intriguing interplay between components. Modelling the optical properties of these represents an important challenge.

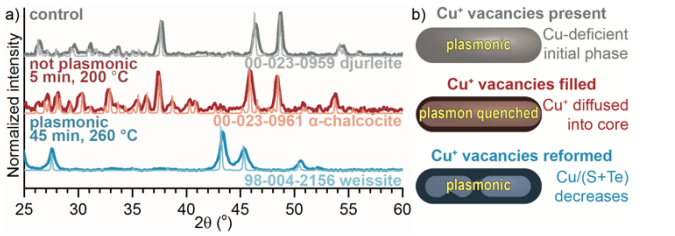

Fig. 4. PXRD (a) of samples with distinct LSPR and a depiction of the transformation (b).

All authors except DPR: Investigation **DPR:** Conceptualization; **KEP:** Conceptualization, all other roles. No conflicts to declare. **Funding:** Dreyfus Foundation (BL-17-004), NSF (DMR-2003337 & MRI-1724948), PSU MRFN program.

Notes and references

1. Y. Zhao and C. Burda, *Energy Environ. Sci.*, 2012, **5**, 5564.
2. S. K. Cushing, J. Li, F. Meng, T. R. Senty, S. Suri, M. Zhi, M. Li, A. D. Bristow, and N. Wu, *J. Am. Chem. Soc.*, 2012, **134**, 15033.
3. J. Cui, Y. Li, L. Liu, L. Chen, J. Xu, J. Ma, G. Fang, E. Zhu, H. Wu, L. Zhao, L. Wang, and Y. Huang, *Nano Lett.*, 2015, **15**, 6295.
4. K. M. Haas and B. J. Lear, *Chem. Sci.*, 2015, **6**, 6462.
5. X. Y. Gan, E. L. Keller, C. L. Warkentin, S. E. Crawford, R. R. Frontiera, and J. E. Millstone, *Nano Lett.*, 2019, **19**, 2384.
6. A. Agrawal, S. H. Cho, O. Zandi, S. Ghosh, R. W. Johns, and D. J. Milliron, *Chem. Rev.*, 2018, **118**, 3121.
7. J. A. Faucheaux, A. L. D. Stanton, and P. K. Jain, *J. Phys. Chem. Lett.*, 2014, **5**, 976.
8. H. Zhang and Y. Xia, *ACS Sens.*, 2016, **1**, 384.
9. W. Li, R. Zamani, P. Rivera Gil, B. Pelaz, M. Ibáñez, D. Cadavid, A. Shavel, R. A. Alvarez-Puebla, W. J. Parak, J. Arbiol, and A. Cabot, *J. Am. Chem. Soc.*, 2013, **135**, 7098.
10. I. Kriegel, C. Jiang, J. Rodríguez-Fernández, R. D. Schaller, D. V. Talapin, E. da Como, and J. Feldmann, *J. Am. Chem. Soc.*, 2012, **134**, 1583.
11. J. M. Luther, P. K. Jain, T. Ewers, and A. P. Alivisatos, *Nat. Mater.*, 2011, **10**, 361.
12. F. Wang, Q. Li, L. Lin, H. Peng, Z. Liu, and D. Xu, *J. Am. Chem. Soc.*, 2015, **137**, 12006.
13. M. Kanehara, H. Arakawa, T. Honda, M. Saruyama, and T. Teranishi, *Chem. Eur. J.*, 2012, **18**, 9230.
14. D. Zhu, A. Tang, H. Ye, M. Wang, C. Yang, and F. Teng, *J. Mater. Chem. C.*, 2015, **3**, 6686.
15. O. Elimelech, J. Liu, A. M. Plonka, A. I. Frenkel, and U. Banin, *Angew. Chem. Int. Ed.*, 2017, **56**, 10335.
16. L. Chen and G. Li, *ACS Appl. Nano Mater.*, 2018, **1**, 4587.
17. I. Kriegel, J. Rodríguez-Fernández, A. Wisnet, H. Zhang, C. Waurisch, A. Eychmüller, A. Dubavik, A. O. Govorov, and J. Feldmann, *ACS Nano.*, 2013, **7**, 4367.
18. O. A. Balitskii, M. Sytnyk, J. Stangl, D. Primetzhofer, H. Groiss, and W. Heiss, *ACS Appl. Mater. Interfaces.*, 2014, **6**, 17770.
19. X. Liu, X. Wang, B. Zhou, W.-C. Law, A. N. Cartwright, and M. T. Swihart, *Adv. Funct. Mater.*, 2013, **23**, 1256.
20. K. H. Hartstein, C. K. Brozek, S. O. M. Hinterding, and D. R. Gamelin, *J. Am. Chem. Soc.*, 2018, **140**, 3434.
21. P. K. Jain, K. Manthiram, J. H. Engel, S. L. White, J. A. Faucheaux, and A. P. Alivisatos, *Angew. Chem. Int. Ed.*, 2013, **52**, 13671.
22. D. Dorfs, T. Härtling, K. Miszta, N. C. Bigall, M. R. Kim, A. Genovese, A. Falqui, M. Povia, and L. Manna, *J. Am. Chem. Soc.*, 2011, **133**, 11175.
23. S. Wang, A. Riedinger, H. Li, C. Fu, H. Liu, L. Li, T. Liu, L. Tan, M. J. Barthel, G. Pugliese, F. De Donato, M. Scotto D'Abbusco, X. Meng, L. Manna, H. Meng, and T. Pellegrino, *ACS Nano.*, 2015, **9**, 1788.
24. L. Guo, D. D. Yan, D. Yang, Y. Li, X. Wang, O. Zalewski, B. Yan, and W. Lu, *ACS Nano.*, 2014, **8**, 5670.
25. N. J. Freymeyer, P. D. Cunningham, E. C. Jones, B. J. Golden, A. M. Wiltrout, and K. E. Plass, *Cryst. Growth Des.*, 2013, **13**, 4059.
26. S. C. Riha, D. C. Johnson, and A. L. Prieto, *J. Am. Chem. Soc.*, 2011, **133**, 1383.
27. I. Kriegel, A. Wisnet, A. R. Srimath Kandada, F. Scotognella, F. Tassone, C. Scheu, H. Zhang, A. O. Govorov, J. Rodríguez-Fernández, and J. Feldmann, *J. Mater. Chem. C.*, 2014, **2**, 3189.
28. S.-W. Hsu, K. On, and A. R. Tao, *J. Am. Chem. Soc.*, 2011, **133**, 19072.
29. A. H. Caldwell, D.-H. Ha, X. Ding, and R. D. Robinson, *J. Chem. Phys.*, 2014, **141**, 164125.
30. M. Ha, J.-H. Kim, M. You, Q. Li, C. Fan, and J.-M. Nam, *Chem. Rev.*, 2019, **119**, 12208.
31. Y. Kim, K. Y. Park, D. M. Jang, Y. M. Song, H. S. Kim, Y. J. Cho, Y. Myung, and J. Park, *J. Phys. Chem. C.*, 2010, **114**, 22141.
32. K. Miszta, R. Brescia, M. Prato, G. Bertoni, S. Marras, Y. Xie, S. Ghosh, M. R. Kim, and L. Manna, *J. Am. Chem. Soc.*, 2014, **136**, 9061.
33. J. C. Flanagan, L. P. Keating, M. N. Kalasad, and M. Shim, *Chem. Mater.*, 2019, **31**, 9307.
34. L. F. Garcia-Herrera, H. P. McAllister, H. Xiong, H. Wang, R. W. Lord, S. K. O'Boyle, A. Imamovic, B. C. Steimle, R. E. Schaak, and K. E. Plass, *Chem. Mater.*, 2021, **33**, 3841.
35. N. Hooshmand and M. A. El-Sayed, *Proc Natl Acad Sci USA.*, 2019, **116**, 19299.
36. M. Lotfipour, T. Machani, D. P. Rossi, and K. E. Plass, *Chem. Mater.*, 2011, **23**, 3032.
37. Y. Liu, T. Ding, X. Luo, Y. Li, J. Long, and K. Wu, *Chem. Mater.*, 2020, **32**, 224.
38. A. Sugathan, B. Bhattacharyya, V. V. R. Kishore, A. Kumar, G. P. Rajasekar, D. D. Sarma, and A. Pandey, *J. Phys. Chem. Lett.*, 2018, **9**, 696.
39. A. Putnis, *Philosophical Magazine.*, 1976, **34**, 1083.
40. I. Jen-La Plante, A. Teitelboim, I. Pinkas, D. Oron, and T. Mokari, *J. Phys. Chem. Lett.*, 2014, **5**, 590.
41. J. L. Fenton, B. C. Steimle, and R. E. Schaak, *Science.*, 2018, **360**, 513.